

Crafting networks to achieve (or not) chaotic states.

Sarah De Nigris* and Xavier Leoncini†

Aix Marseille Université, Université de Toulon, CNRS, CPT UMR 7332, 13288 Marseille, France

(Dated:)

The influence of networks topology on collective properties of dynamical systems defined upon it is studied in the thermodynamic limit. A network model construction scheme is proposed where the number of links, the average eccentricity and the clustering coefficient are controlled. This is done by rewiring links of a regular one dimensional chain according to a probability p within a specific range r , that can depend on the number of vertices N . We compute the thermodynamical behavior of a system defined on the network, the XY -rotors model, and monitor how it is affected by the topological changes. We identify the network dimension d as a crucial parameter: topologies with $d < 2$ exhibit no phase transitions while ones with $d > 2$ display a second order phase transition. Topologies with $d = 2$ exhibit states characterized by infinite susceptibility and macroscopic chaotic/turbulent dynamical behavior. These features are also captured by d in the finite size context.

PACS numbers: 05.20.-y, 05.45.-a

Networks are ubiquitous in the reality surrounding us and indeed the network perspective for systems of interacting agents has been a real paradigm shift in various realms ranging from physics to biology, sociology and economics [1–4]. One pivotal feature shared by many existing networks, like the World Wide Web [5–7] or social networks [8], is the so called ‘small-world’ property: two nodes are separated by a short path consisting in just few edges thanks to the presence of long-range connections, the *shortcuts*, in the network. Since this property often arises in a self-organized fashion, it could seem natural at first to infer that those shortcuts favor the flow of information and more easily lead to collective states, like if a kind of evolutionary principle is at play. But are indeed those long-range links always beneficial to enhance global coherence? A striking example of this dilemma can be the brain: from one side it displays the small-world property [9] but, at the same time, there are evidences of *chaotic* response in living neural systems [10]. In contrast, small-world topologies can be a fertile substrate to enhance transport phenomena as navigation [11] and, more recently, it has also been shown that the overall conductance of a network is advantaged by the introduction of long-range links [12]. It hence appears highly non trivial, when dealing with interacting agents upon a network, to ask oneself what kind of collective behavior they can possibly display since a chaotic response can arise along with a coherent one due to the presence of long-range links.

This work inscribes itself in this frame: we provide here a mean to construct a class of networks in which the addition of long-range links can give rise to a whole range of dynamical and statistical behaviors and, in particular, it also entails a chaotic state of infinite susceptibility, similar to the one encountered in [13, 14]. Moreover our

network model is crafted to embed real networks characteristics but via minimal assumptions so to ensure a certain form of simplicity. As we will display in the following, we related the different behaviors to the network *dimension*, which changes according to the injection of long-range links.

In our model, networks are built starting from a one dimensional ring with periodic boundary conditions and a uniform degree $k \propto N^{\gamma-1}$ ($1 \leq \gamma \leq 2$) (where N is the number of vertices), which constitutes the backbone. In this work, we set γ close to 1, $\gamma = 1.2$, in order to have a few links per vertex (for instance we get $k = 12$ for $N = 2^{14}$). We then proceed to a construction similar to the Watts-Strogatz one for Small World networks [15]: we rewire each link with probability p but, differently from [15], we impose to rewire it within a range r (Fig. 1). Therefore with our parameters (γ, p, r) we put three ingredients meant to mimic concrete systems: first the condition of *sparseness* through γ , i.e. a very low vertex degree compared to the system size [4], second we introduced the concept of *interaction range* constraining the links to be at most of a fixed length r and last we inject *randomness* in the structure so to have a non uniform degree. Hence, from one side, the range parameter r mimics the fact that in many natural and artificial systems interactions can occur only within a certain neighborhood and on the other side the probability p ensures the presence of randomness in the link distribution, so that all the length scales occur. The range concept is reminiscent of the Kleinberg model [16] but, in our case, the choice of r entails a sharp cutoff in the distribution of the accessible link lengths and, moreover, the probability p to rewire a link within the range r is uniform. The range constraint allows a control on the dimension: heuristically we can forecast that if we choose for instance $r \propto \sqrt{N}$, the more links are rewired (i.e. for high p), the more the network will be shaped like a bi-dimensional object, because we have in some sense crafted from the initial ring a $\sqrt{N} \times \sqrt{N}$ lattice. To give a more quantita-

* denigris.sarah@gmail.com

† Xavier.Leoncini@cpt.univ-mrs.fr

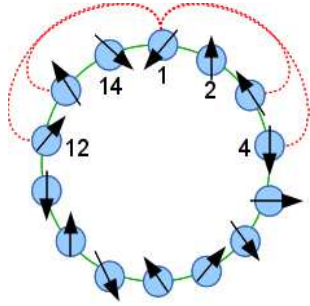


Figure 1. (color online) Practical network construction for $N = 14$, $\gamma = 1.2$ thus $k \propto \lfloor N^{0.2} \rfloor = 2$ and $r = \lfloor \sqrt{N} \rfloor = 3$. The starting configuration is the solid (green) line since we have just two links per spin and the dotted (red) links are the possible rewiring.

tive counterpart to this view, we define the dimension d similarly to the dimension on Euclidean lattices: for the latter, it holds a power law relation between the volume and a characteristic length $V \propto r^d$, the exponent d being the dimension. Then in our context of networks, we have to consider a specific length scale. Here we settled for the average of the vertices eccentricity $ec(i)$, i.e. the longest path $\ell_{i,j}$ $i \neq j$ attached to each vertex i . Thus we define our characteristic length ℓ as:

$$\ell = \frac{1}{N} \sum_i ec(i). \quad (1)$$

Hence if we consider its scaling with the network volume (size) N , we obtain a definition of dimension:

$$d = \frac{\log N}{\log \ell}, \quad (2)$$

The definition in Eq. (2) recovers in the $N \rightarrow \infty$ limit the one already proposed in [17–19] in which they consider the power law scaling of the average path length ℓ_{av} with the network size N , while we take in account in Eq. (1) the average vertex eccentricity ℓ_{ec} . These two quantities are indeed related since $\ell_{ec} \sim 2\ell_{av}$ and this assumption was also numerically tested. It is hence evident that the difference between the two dimension definitions is a term vanishing logarithmically with the size N , thus proving their equivalence in the $N \rightarrow \infty$ limit. However, in the range of system sizes used in our simulations, the definition in Eq. (1) was the more suitable choice to grasp the dimension since the aforementioned difference is still important enough to introduce a small shift in the dimension value. In Eq. (2), it is straightforward to see that the dimension of the completely rewired ($p = 1$) configuration is intrinsically related to the range r : indeed for $p = 1$, we have that $\ell \sim N/r$ since each node very probably possesses a link rewired at a distance r . Therefore, if $\ell \sim N/r$, we have that Eq. (2) becomes

$$d_r = \frac{\log N}{\log N - \log r}. \quad (3)$$

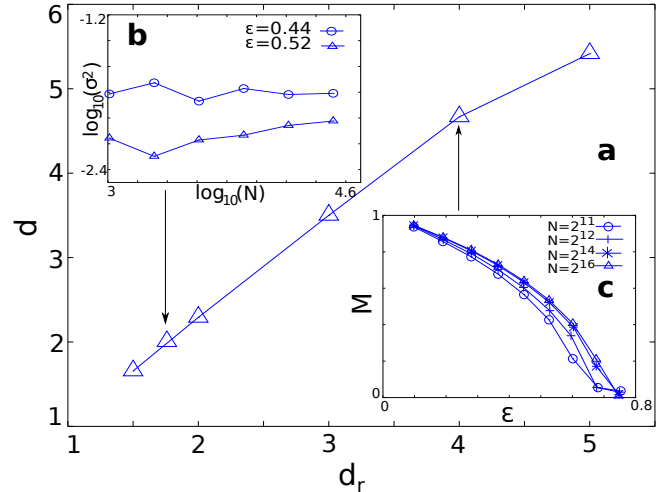


Figure 2. (color online) (a) Dimension of a completely rewired network ($p = 1$) with $N = 2^{14}$ and $r \propto N^\delta$. The horizontal axis is the parametrization in Eq. (3) which gives, with our choice of r , $d_r = 1/(1 - \delta)$. (b) Scaling of the magnetization variance $\sigma^2(N)$ with the system size N for $d = 2$. (c) Phase transition of the magnetization $M(\epsilon)$, $\epsilon = E/N$ for $d > 4$. The error bars are within the dots size.

In what follows we shall use the dimension d_r given by Eq. (3) as our control parameter: in practice d_r corresponds to a re-parametrization of the range which we will consider to be of the type $r \sim N^\delta$ with ($N \gg 1$ and $\delta > \gamma$). If we take our previous example of $r = \sqrt{N}$, we obtain that the corresponding network with $p = 1$ has indeed $d_r = 2$ and, in Fig. 2(a), we display how the measured network dimension for $p = 1$ follows Eq. (3) so that, fixing the range $r(N)$, we can control the resulting dimension once we have rewired all the links, independently from the size.

Having thus an operative and general way to set and quantify the dimension, we used our network model to investigate the thermodynamic response of a dynamical system defined upon these networks and test the influence of the dimension d in Eq. (2). With this goal in mind, we consider N XY -rotors [20, 21], whose dynamics is described by an angle $\theta_i(t)$ and its canonically associated momentum $p_i(t)$. We shall show that the rewiring of a few links, beyond altering significantly the network structure, can also entail different collective behaviors: in particular, we shall investigate if, like on regular lattices, we have a spontaneous symmetry breaking for $d > 2$, which is absent when $d < 2$. This brings some analogies to the extension of the Mermin-Wagner theorem on inhomogeneous structures [22, 23] in which the critical parameter to discriminate between different regimes is the spectral dimension [24–26], therefore opening an interesting thread of research. Moreover we shall focus on $d = 2$, or $r \sim \sqrt{N}$, to see if a chaotic state emerges, displaying some similarities with the one observed in the regular structure discussed in [13]. Returning back to the XY -rotors, each rotor i is located on a network vertex

and its interactions are provided by the set V_i of vertices attached to it via the links. The Hamiltonian of the system reads:

$$H = \sum_{i=1}^N \frac{p_i^2}{2} + \frac{J}{2 \langle k \rangle} \sum_{i \in V_i} (1 - \cos(\theta_i - \theta_j)), \quad (4)$$

where $J > 0$, $\langle k \rangle$ is the average degree and $V_i = \{j \neq i \mid \exists e_{i,j} \in E\}$, E being the ensemble of edges. The dynamics of the network is given by the two Hamilton equations:

$$\begin{cases} \dot{\theta}_i = p_i \\ \dot{p}_i = -\frac{J}{\langle k \rangle} \sum_{j \in V_i} \sin(\theta_i - \theta_j) \end{cases}, \quad (5)$$

We run molecular dynamics (MD) simulations of the isolated system in Eqs. (5), starting with Gaussian initial conditions for $\{\theta_i, p_i\}$. The simulations are performed integrating the dynamic equations in Eqs. (5) with the fifth order optimal symplectic integrator, described in [27], with a time step of $\Delta t = 0.05$. Such an integrating scheme allows us to check the correctness of the numerical integration since we verified at each time step that the conserved quantities of the system, the energy $E = H$ and the total momentum $P = \sum_i p_i / N$, are effectively constant. The total momentum P is set at 0 as initial condition without loss of generality. In order to grasp the amount of coherence in the system, we define a magnetization $M = |\mathbf{M}|$ as order parameter:

$$\mathbf{M} = \frac{1}{N} \sum_i (\cos \theta_i, \sin \theta_i) \quad (6)$$

and, once the system has reached a stationary state, we measure \overline{M} , where the bar stands for the temporal mean. Thus, in the stationary state, if $\overline{M} \sim 1$, all the rotors point in the same direction, whereas if $\overline{M} \sim 0$ there is not a preferred direction. Practically, once the network topology and the size N are fixed, we monitor the average magnetization $\overline{M}(\varepsilon, N)$ for each energy $\varepsilon = E/N$ in the physical range. We perform the temporal mean on the second half of the simulation, after checking that the magnetization has reached a stationary state, when it is reached (i.e. not in the case of the chaotic state). The simulations time is typically of order $Tf = 10^4 - 10^5$. In the insets of Fig. (2) we display the dynamical response of the XY model to different dimensions: we chose r so to have $d = 2$ for $r \propto \sqrt{N}$ and $d > 4$ for $r \propto N^{3/4}$. For the latter, in Fig. (2)c the magnetization displays a second order phase transition, seeming to occur at $\varepsilon = E/N \sim 0.75$, in the same fashion of the Hamiltonian Mean Field (HMF) model [28]. It is noteworthy that, for the XY model, the dimension 4 is the one at which mean field theory starts to apply and, indeed, the phase transition displayed in Fig. 2(c) for $d > 4$ seems to confirm this picture. For the case with $d = 2$ we observed a state similar to the one described in [13, 14]: the magnetization, for low energy densities $\varepsilon = E/N$, is

affected by important fluctuations like if the order parameter was oscillating between the mean field value and zero. Moreover this regime does not reach the equilibrium on the timescales considered: its persistence was checked for simulation times $Tf \sim 10^6$, i.e. 10 times longer than in previous cases and nevertheless it was not possible to observe its relaxing. To give further insights on this chaotic state arising in the network with $d = 2$, we looked at the magnetization variance $\sigma^2 = (\overline{M} - \overline{\overline{M}})^2$, where the bar stands again for the temporal mean, in order to give a quantitative measure of this regime. As shown in Fig. 2(b) the variance is unaffected by the size: this flat profile is in striking contrast with the variance's canonical scaling $\sigma^2 \propto 1/N$, leading to vanishing fluctuations in the thermodynamic limit. On the contrary, if we take into account the definition of the magnetic susceptibility

$$\chi \sim \lim_{N \rightarrow \infty} N \sigma^2, \quad (7)$$

we have that this regime shall be characterized by an infinite susceptibility in the thermodynamic limit. The peculiar nature of this regime is also highlighted by its persistence in an energy range. Indeed in the usual XY Kosterlitz-Thouless transition the divergence of the susceptibility occurs at the phase transition point [29], while these "turbulent" states exist in a whole interval energies up to the critical one. In fact these states are somewhat reminiscent of the observed *quasi-stationary states* (QSS) occurring in the Hamiltonian Mean Field model or more generally in systems with long range interactions [30–34]. Nevertheless, as mentioned, we do not observe any relaxation in contrast with the QSS's behaviour.

Our model brings interesting perspectives for finite size systems as well: as a first observation, we should note that our construction procedure, like the Watts-Strogatz algorithm for Small World networks [15], induces on average $N_R = Nkp \propto N^\gamma p$ rewired links. Hence the fraction of long-range connections increases with the size (in the present study very slightly because of our choice $\gamma = 1.2$). We thus argue the existence of a non trivial interplay between p , r and N , so that it is possible, like for Small World networks, to tune p in order to change the measured dimension for a given size N . In some sense, d can turn out to be, for a finite size system, a measure of an *effective dimension* produced by the fraction of rewired links. To test our hypothesis, we consider $N = 2^{14}$ and $N = 2^{16}$ and in Fig. 3(a)-(d) we show how the progressive introduction of long-range links in the network drags the dimension to $d = 2$ for $r = \sqrt{N}$ (Fig. 3(a)) and to $d = 4$ for $r = N^{3/4}$ (Fig. 3(d)). Indeed the shift between the two dimension curves mirrors the effect of the two sizes and it is more pronounced for the largest range $r = N^{3/4}$. Therefore a natural question arises: does the dynamical behavior relate to this "finite size" dimension? Similarly to what we did in Fig. 2, we analyzed the dynamical response of the XY -model and Fig. 3, we display our results for $r \sim \sqrt{N}$ and $r \sim N^{3/4}$. To guide our investigation, we can use Fig. 3(a)-(d) as a map to locate the

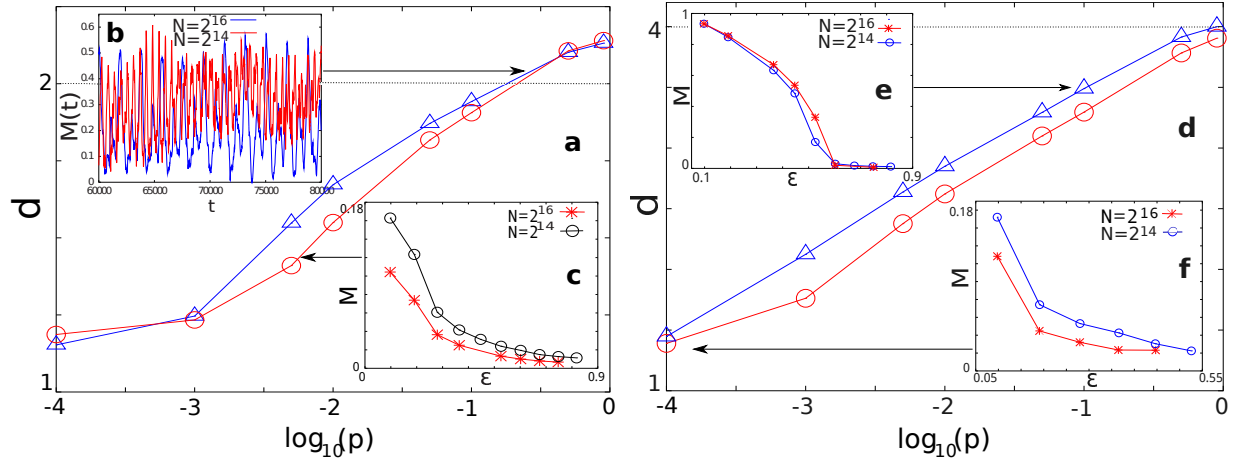


Figure 3. (color online) Dimension and its influence on global coherence. The relation between the dimension d and the fraction of links rewired, given by p , for (a) $r = \sqrt{N}$ and (d) $r = N^{3/4}$ for two network sizes, $N = 2^{14}$ (dots) and $N = 2^{16}$ (triangles). In (a) the dimension shifts from 1 to 2, whereas in (d) the increased r drags the dimension up to 4. In the insets we display the corresponding thermodynamical response: in (b) for a network with $d = 2$ the magnetization shows a chaotic behavior at $\varepsilon = 0.350(1)$ while in (c) and (f) the quasi-unidimensional network does not sustain any long-range order, entailing the vanishing of the magnetization for every energy. Finally, for $d \simeq 3$, (e) shows a second order phase transition at $\varepsilon_c = 0.6$. For the magnetization equilibrium values (c,e,f) and the dimension (a,d), the error bars are within the dots size.

parameter zones characterized by different dimensions. Focusing first on $r \sim \sqrt{N}$, we chose the probabilities so to have either a network with $d = 2$, $p = 0.1$ and $p = 0.3$, or an quasi one-dimensional one, $p = 0.005$. In Fig. 3(b) we show that indeed these networks generate a chaotic state similar to the one in Fig. 2(a) and described in [13, 14]: the heavy oscillations of the magnetization do not relax even for long time simulations and their amplitude (i.e. the variance) is unaffected by the size increase. This peculiar state, appearing for low energy densities, seems again intrinsically related to the dimensionality since the two aforementioned probabilities values entail $d \sim 2$, as displayed by Fig. 3(a). Moreover we considered several sizes to investigate the impact of the size increase and, again, there is any significant difference between $N = 2^{14}$ and $N = 2^{16}$ in the fluctuations amplitude. Nevertheless it is noteworthy to observe a signature of the different sizes in the oscillations period, which is significantly slower in the $N = 2^{16}$ case. This effect, entangling system size and timescales, can be reminiscent with the lifetime of QSSs [30–34] of the HMF model. This analogy, along with aforementioned one concerning the phase transition, points to very interesting research perspectives to shed light on the connection between these two systems. Continuing in our analysis, for $p = 0.005$ which gives $d \lesssim 1.7$ (Fig. 3(a)), the magnetization vanishes for all the energies, so to confirm the crucial role played by the crossover to the two dimensional configuration. Taking now into account the case $r \sim N^{3/4}$, we show in Fig. 3(e) that the system undergoes a second order phase transition, as it happens in Fig. 2(c) when $d > 2$. On the other hand, the short-range regime is at play for lower probabilities in Fig. 3(f)

where we display the vanishing of the order parameter for $d \leq 1.5$. In conclusion, we have provided a way to construct a class of networks whose dimension d is controllable via the range parameter r . We have shown how this dimension, in the thermodynamic limit, is related to different collective states of the XY model upon those networks: for $d > 2$ the system displays a second order phase transition which becomes very similar to the one of the HMF model for $d > 4$, while for $d = 2$ a regime characterized by an infinite susceptibility is at play. Beyond the analysis in the thermodynamic limit, we also interpreted the dimension d in the case of finite size systems: in this frame d is a function of (N, r, p) so that we can “adjust” the probability of rewiring p to obtain the desired *effective dimension*. Considering the evidences we have displayed, we may argue that, for general networks, the considered dimension can be a key topological characteristic that in the end governs the final collective behavior of large coupled systems. Moreover we believe that the peculiar case of networks with $d = 2$, for which the chaotic collective state emerges, could lead to many interesting applications: for instance, the infinite susceptibility could be used to amplify signals, or a better understanding of the dynamics could prove useful in the context of modeling and studying turbulent behaviors in an isolated system.

ACKNOWLEDGEMENTS

The authors are grateful to the Referee for having pointed Refs. [22–25]. S. d. N. is supported by DGA/MRIS, X. L. is partially supported by the FET project Multiplex 317532.

[1] S. N. Dorogotsev, *Evolution of Networks: from Biological Nets to the Internet and WWW* (Oxford University Press, Oxford, 2003).

[2] M. E. J. Newman, *Networks: An Introduction* (Oxford University Press, 2010).

[3] S. Havlin and R. Cohen, *Complex Networks: Structure, Robustness and Function* (Cambridge Univ. Press, 2010).

[4] A. Barrat, M. Barthelemy, and A. Vespignani, *Dynamical processes on complex networks* (Cambridge Univ. Press, 2008).

[5] A. Broder, R. Kumar, F. Maghoul, P. Raghavan, S. Rajagopalan, R. Stata, A. Tomkins, and J. Wiener, *Computer Networks* **33**, 309 (2000).

[6] R. Albert, H. Jeong, and A.-L. Barabási, *Nature* **401**, 130 (1999).

[7] A.-L. Barabási, R. Albert, and H. Jeong, *Physica A: Statistical Mechanics and its Applications* **281**, 69 (2000).

[8] J. Travers and S. Milgram, *Sociometry* **32**, 425 (1969).

[9] E. Bullmore and O. Sporn, *Nature Reviews Neuroscience* **10**, 186 (2009).

[10] W. J. Freeman, *IJBC* **2**, 451 (1992).

[11] J. M. Kleinberg, *Nature* **406**, 845 (2000).

[12] C. L. N. Oliveira, P. A. Morais, A. A. Moreira, and J. S. Andrade, *Phys. Rev. Lett.* **112**, 148701 (2014).

[13] S. De Nigris and X. Leoncini, *EPL* **101**, 10002 (2013).

[14] S. De Nigris and X. Leoncini, *Phys. Rev. E* **88**, 012131 (2013).

[15] D. J. Watts and S. H. Strogatz, *Nature* **393**, 440 (1998).

[16] J. M. Kleinberg, in *Proceedings of the Thirty-second Annual ACM Symposium on Theory of Computing*, STOC '00 (ACM, New York, NY, USA, 2000) pp. 163–170.

[17] S. Havlin and A. Bunde, *Springer, London* (Springer, 1991).

[18] G. Baglietto, E. V. Albano, and J. Candia, *J. Stat. Phys.*, 1 (2013).

[19] M. E. J. Newman and D. J. Watts, *Phys. Rev. E* **60**, 7332 (1999).

[20] J. J. Binney, N. J. Dowrick, A. J. Fisher, and M. E. J. Newman, *The Theory of Critical Phenomena: An Introduction to the Renormalization Group* (Oxford University Press, 1992).

[21] P. M. Chaikin and T. C. Lubensky, *Principles of Condensed Matter Physics* (Cambridge Univ. Press, 1995).

[22] D. Cassi, *Phys. Rev. Lett.* **68**, 3631 (1992).

[23] R. Burioni and D. Cassi, *Phys. Rev. Lett.* **76**, 1091 (1996).

[24] R. Burioni, D. Cassi, and A. Vezzani, *Phys. Rev. E* **60**, 1500 (1999).

[25] R. Burioni, D. Cassi, and C. Destri, *Phys. Rev. Lett.* **85**, 1496 (2000).

[26] R. Burioni and D. Cassi, *Journal of Physics A: Mathematical and General* **38** (2005).

[27] R. I. McLachlan and P. Atela, *Nonlinearity* **5**, 541 (1992).

[28] A. Campa, T. Dauxois, and S. Ruffo, *Phys. Rep.* **480**, 57 (2009).

[29] J. M. Kosterlitz and J. D. Thouless, *J. Phys. C: Solid State Phys.* **6** (1973).

[30] W. Ettoumi and M.-C. Firpo, *J. Phys. A: Math. Theor.* **44**, 175002 (2011).

[31] W. Ettoumi and M.-C. Firpo, *Phys. Rev. E* **87**, 030102(R) (2013).

[32] P.-H. Chavanis, G. De Ninno, D. Fanelli, and S. Ruffo, “Out-of-equilibrium phase transitions in mean-field hamiltonian dynamics,” in *Chaos, Complexity and Transport: Theory and applications*, edited by C. Chandre, X. Leoncini, and G. M. Zaslavsky (World Scientific, 2008) pp. 3–26.

[33] T. L. Van Den Berg, D. Fanelli, and X. Leoncini, *EPL* **89**, 50010 (2010).

[34] Y. Levin, R. Pakter, F. B. Rizzato, T. N. Teles, and F. P. Benetti, *Phys. Rep.* **535**, 1 (2014).